ARTICLE NO. 78-516R

Effect of Prebuckling Deformations on Buckling of Laminated Composite Circular Cylindrical Shells

Robert M. Jones* and Jose C.F. Hennemann†
Southern Methodist University, Dallas, Texas

Laminated composite materials are rapidly replacing metals in contemporary shell applications. Thus, the structural behavior of such shells must be predicted, and, in particular, we must be able to predict the buckling behavior. The orthotropy of the fiber-reinforced laminae and the composition of the laminae lead to coupling stiffnesses between forces and changes in curvature as well as between moments and in-surface strains. These coupling stiffnesses do not occur for isotropic shells except when the boundary supports are not in the middle surface. The effect of prebuckling deformations for isotropic shells is to lower the actual buckling load below the classical buckling load by up to 20% for some loading and boundary conditions. The effect of prebuckling deformations on the axial and lateral pressure buckling loads of circular cylindrical shells made of fiber-reinforced composite laminates is found to decrease as the orthotropy increases and as the laminate coupling stiffnesses decrease. Variations in the elastic and geometric parameters are studied for both antisymmetric and unsymmetric laminates. Generally, the effect of prebuckling deformations is far less important for laminated shells than for isotropic shells.

Nomenclature

A_{ij},B_{ij},D_{ij}	= laminate extensional, coupling, and bending stiffnesses[1]
E_1,E_2	= Young's moduli in lamina principal material directions
G_{12}	= shear modulus in the lamina 1-2 plane
L	= length of shell
$\bar{N}$	= axial load per unit width
n	= number of circumferential buckle waves
p	= external lateral pressure
$p_0(P_0)$	= classical lateral pressure (axial compression) buckling load for an orthotropic shell (no coupling between bending and extension)
P	= axial load
r	= radius of shell midsurface
t	= thickness of shell
u,v,w	= shell midsurface displacements (Fig. 2)
x,y,z	= coordinates of shell midsurface (Fig. 2)
ν_{ij}	= Poisson's ratio for contraction (expansion) in the j direction due to tension (compression) in the i direction

Subscript

CL	= classical value for membrane prebuckling state

Introduction

A PROMINENT characteristic of laminated fiber-reinforced shells is the coupling between bending and extension that results when the laminate is not symmetric about the shell middle surface. This coupling characteristic was studied by Jones and Morgan for shell buckling and vibration problems[2] and by Whitney and Leissa for plate deflection, buckling, and vibration problems[3,4] as well as by many other investigators. However, the coupling is included only in the buckling equations and is ignored in the equations governing the prebuckling behavior. That is, a shell is assumed to expand uniformly as a membrane as shown in Fig. 1, and the conditions at the shell edge are ignored. Classical buckling loads from that membrane state are calculated. In contrast to the membrane prebuckling deformation, the actual or rigorous prebuckling deformations that satisfy the boundary conditions at the end of the shell are also shown in Fig. 1. The curvature and stresses corresponding to the actual deformations prior to buckling can be either stabilizing or destabilizing influences on the buckling behavior. For isotropic shells, Stein[5] and Almroth[6] show that rigorous consideration of boundary conditions at the shell edges results in buckling loads that are smaller than if prebuckling boundary conditions are ignored. However, the boundary condition induced prebuckling curvature does not appear to result in reductions of buckling loads from classical buckling theory in sufficient magnitude to predict accurately the measured buckling loads.[6]

The effect of coupling induced prebuckling curvature on shell buckling loads has not been investigated and could be more significant than boundary condition induced

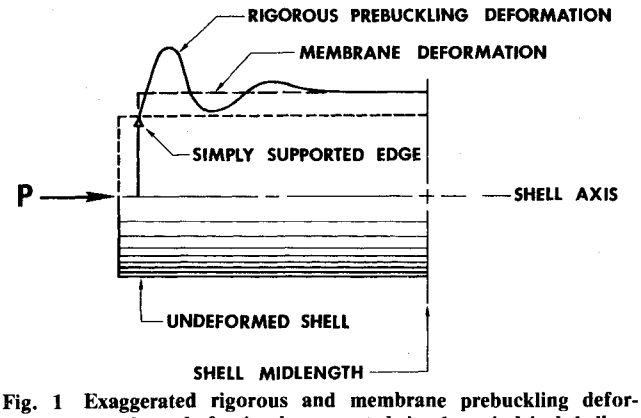

Fig. 1 Exaggerated rigorous and membrane prebuckling deformations near the end of a simply supported circular cyindrical shell.

Presented as Paper 78-516 at the AIAA/ASME 19th Structures, Structural Dynamics, and Materials Conference, Bethesda, Md., April 3-5, 1978; submitted Feb. 8, 1978; revision received June 25, 1979.

Index categories: Structural Stability; Structural Statics; Structural Composite Materials.

*Professor of Solid Mechanics. Associate Fellow AIAA.

†Graduate Student. Now Assistant Professor of Civil Engineering, Universidade Federal do Rio Grande do Sul, Porto Alegre, Brazil.

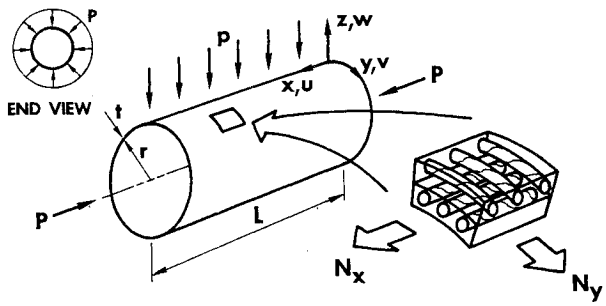

Fig. 2 Cross-ply laminated circular cylindrical shell under axial and lateral pressure.

prebuckling curvature. There is no direct basis for estimating the significance of coupling induced prebuckling curvature on shell buckling loads. For plates, the coupling induced buckling curvatures result in reductions of buckling loads of up to 70% from symmetrically laminated configurations. For shells, the analogous reduction is about 65%. For isotropic (or symmetrically laminated) plates, prebuckling boundary conditions are immaterial or trivial because the plate is always flat prior to buckling (unless the plate is not perfectly flat before load is applied). For unsymmetrically laminated plates, no one has, to the authors' knowledge, studied the influence of prebuckling curvature on buckling loads.

The objective of the present paper is to examine the effect on shell buckling loads of prebuckling curvatures induced by coupling between bending and extension due to laminate asymmetry. Curiously, none of the computer programs in which this effect has been incorporated for the past 10 years has been exercised to study the problem. The specific shell studied here is the cross-ply laminated circular cylindrical shell subjected to combinations of axial load and lateral pressure as in Fig. 2. There, the shell geometry is displayed along with the cross-ply laminate with fibers oriented either in the axial or circumferential direction of the cylinder.

The paper is divided into two sections: Theory and Numerical Results. The Theory section is a description of the derivation of the pertinent equilibrium and buckling equations and their solution. In the Numerical Results section, plots of axial or lateral pressure buckling loads relative to the classical buckling loads are presented. The cases discussed include various orthotropic and antisymmetrically laminated cross-ply shells.

Theory

The theoretical basis of this paper is developed in four steps: 1) prebuckling equilibrium equations, 2) solution of prebuckling equilibrium equations, 3) buckling equations, and 4) solution of buckling equations for the buckling loads. The specific derivation of the equilibrium equations and their exact solution along with the derivation of the buckling equations and their solution by a finite-difference approach is described briefly by Jones and Hennemann[7] and in detail by Hennemann.[8] Those equations for cross-ply laminated circular cylindrical shells are generalizations of Almroth's equations for isotropic circular cylindrical shells[6] and specializations of the Bushnell et al.[9] equations for shells of revolution with various wall constructions. Despite the availability for more than 10 years of several computer programs for treatment of the present problem (e.g., BOSOR,[9] SRA,[10] KSHELL,[11] and STAR[12]), not one has been used to obtain numerical results in a definitive study.

In the theoretical developments behind this paper, Donnell's large deflection equilibrium equations[6] and von Kármán's nonlinear strain-displacement relations[13] are adopted in the fashion of Almroth.[6] We solve those equations exactly for the axisymmetric prebuckling radial displacements corresponding to simply supported and clamped edges. Then, we use the adjacent equilibrium method[14] to derive the buckling equations which are a coupled set of homogenous partial differential equations. Separation of variables is used to accomplish reduction to a system of coupled homogenous ordinary differential equations which have nonconstant coefficients because of the nonuniform prebuckling displacements. This system of equations cannot be solved in closed form, so we employ a finite-difference approach used by Almroth[6] to obtain a system of homogenous algebraic equations. Finally, the buckling load is found to occur when the determinant of the matrix of coefficients of the algebraic equations is zero. The accuracy of the buckling load is determined by the number of finite-difference stations and by the accuracy of the interval halving procedure used to find where the determinant is zero.

Numerical Results

Introduction

We will make a numerical comparison of two different buckling loads for circular cylindrical shells with a set of simply supported edge boundary conditions. Two distinct prebuckling states are considered: rigorous prebuckling displacements and membrane prebuckling displacements. The buckling load from a membrane prebuckling state is called the classical buckling load. To get that load, we account for coupling between bending and extension during buckling, but not prior to buckling. For simplicity, we call the buckling load from the actual prebuckling state just the buckling load. The comparisons are made for various numbers of layers in the laminate, elastic properties (E_1/E_2, G_{12}/E_2, and ν_{12}), and geometric parameters (L/r and r/t). The results have been verified to agree with Almroth's results for isotropic shells.[6] We examine orthotropic shells here as well as antisymmetric cross-ply laminated shells.

We choose S2 simply supported edge boundary conditions‡ because of the ready availability of a convenient computer program, BOLS II, for the prediction of buckling loads from a membrane prebuckling state.[2] Moreover, S2 boundary conditions are usually regarded as a lower bound on the buckling of practically supported shells. Thus, S2 boundary conditions are often used in design analysis. Other boundary conditions could be studied, but, as we will see, the need to study them might not be great. That is, we will see that the effects of prebuckling deformations do not lead to large differences from the classical buckling predictions in which prebuckling deformations are ignored.

We present the results as relative axial buckling loads (P/P_{CL}) and relative lateral pressure buckling loads (p/p_{CL}) where the actual buckling loads are normalized by the respective classical buckling loads. A finite-difference mesh with 65 points is sufficient to attain three significant figure accuracy on a CDC CYBER-72 computer.

Orthotropic Shells

We consider orthotropic circular cylindrical shells composed of a single orthotropic layer whose principal material directions are oriented in the axial and circumferential directions of the shell. No coupling stiffnesses B_{ij} exist in the force- and moment-strain-curvature relations. However, the presence of orthotropy will lead us to results that are important in the evaluation of laminated shell buckling results.

Axial Load

The relative axial buckling loads are plotted as a function of the orthotropy ratio E_1/E_2 for a short shell ($L/r = 0.7$) in Fig.

‡S2 boundary conditions are $\delta w = 0$, $\delta M_x = 0$, $\delta N_x = 0$, and $\delta v = 0$, wherein the notation δ is used to indicate that we deal with the first variation during buckling of the respective displacement, force, or moment.

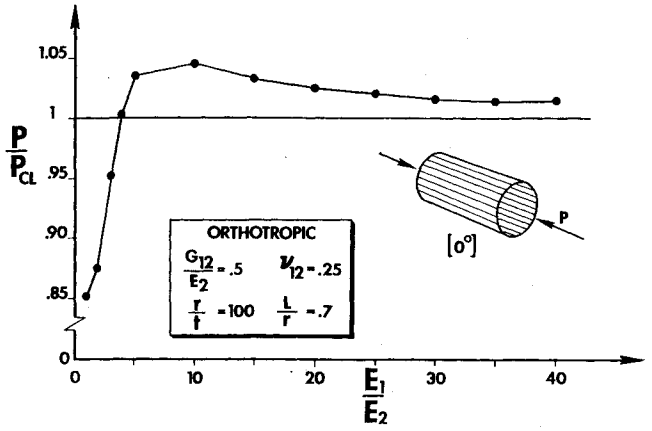

Fig. 3 Relative axial buckling loads as a function of E_1/E_2 for orthotropic shells with fibers oriented in the axial direction.

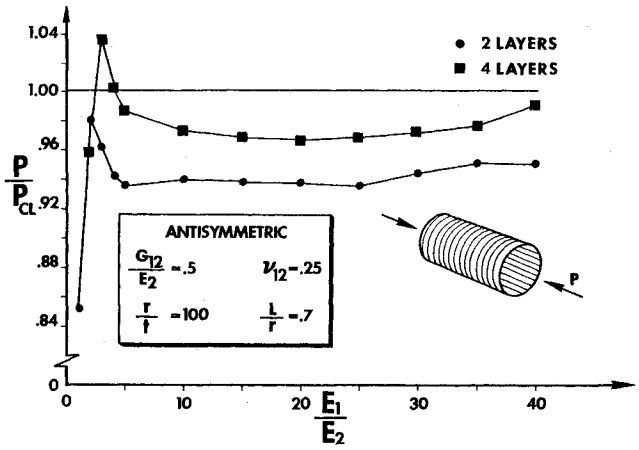

Fig. 4 Relative axial buckling loads as a function of E_1/E_2 for short, antisymmetrically laminated shells.

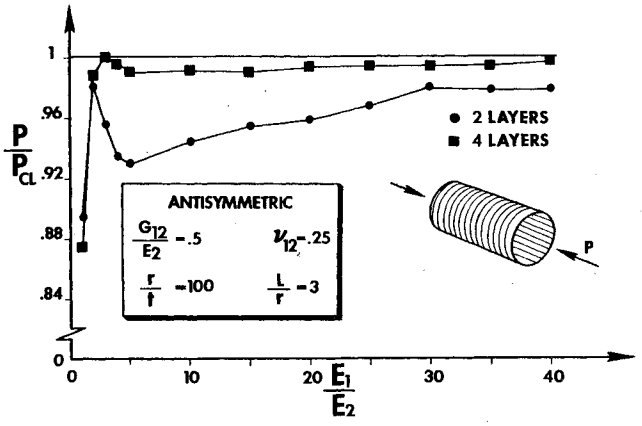

Fig. 5 Relative axial buckling loads as a function of E_1/E_2 for long, antisymmetrically laminated shells.

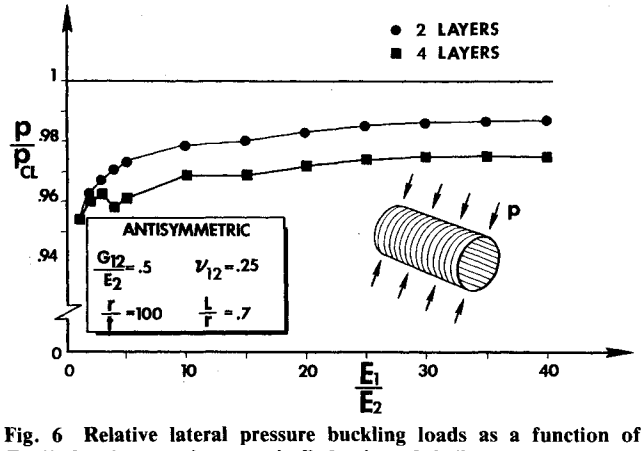

Fig. 6 Relative lateral pressure buckling loads as a function of E_1/E_2 for short, antisymmetrically laminated shells.

3. There, we see that the buckling loads are up to 5% bigger and as little as 15% smaller than the corresponding classical buckling loads. As E_1/E_2 approaches 1, the isotropic shell results of Almroth[6] are approached approximately but not exactly, because $G_{12}/E_2 = 0.5$ and $\nu_{12} = 0.25$ are not possible for isotropic materials. If the fibers are oriented in the circumferential direction, the same behavior as that shown in Fig. 3 exists, but the buckling loads are only about 2% above the classical buckling loads. The relative buckling loads decrease smoothly toward one for increasing E_1/E_2.

Lateral Pressure

Results for buckling under lateral pressure of orthotropic shells with fibers in the axial direction and with fibers in the circumferential direction are different from each other and from results for axial load. The lateral pressure loads are always lower than the classical loads, but approach the classical loads as E_1/E_2 increases. The relative loads for shells with fibers in the axial direction first decrease from the $E_1/E_2 = 1$ result of 0.95 to about 0.90 at $E_1/E_2 = 5$ and then increase to 1. On the other hand, the relative loads for shells with fibers in the circumferential direction increase monotonically and rapidly from 0.95 to 1 as E_1/E_2 increases from 1. Thus, irrespective of loading and direction of largest modulus, the difference between the buckling load and the classical buckling load decreases with increasing orthotropy ratio. This decrease occurs without having any coupling stiffnesses B_{ij}.

Antisymmetric Cross-Ply Laminated Shells

Introduction

A regular antisymmetric cross-ply laminate consists of an even number of orthotropic laminae of the same thickness laid on each other with the directions of the stiffest principal material properties alternating at 0 deg and 90 deg to the laminate x axis. For unidirectional fiber-reinforced laminae, the fiber direction alternates at 0 deg and 90 deg to the x axis. Only the coupling stiffnesses B_{11} and B_{22} exist for these cross-ply laminates, and they can be shown to decrease rapidly to zero as the number of layers increases.[1] However, B_{11} and B_{22} depend strongly on E_1/E_2, so we examine the relative buckling loads as a function of E_1/E_2. We also investigate the influence on the buckling loads of variations in G_{12}/E_2, ν_{12}, L/r, r/t, and the number of layers.

Variation in E_1/E_2

The relative axial buckling loads for variations in E_1/E_2 are shown for two- and four-layered, short ($L/r = 0.7$) and long ($L/r = 3$) shells in Figs. 4 and 5. There, we see that as the number of layers increases, the buckling load approaches the classical solution (this observation is further supported with more numerical results not shown). For two layers, the largest difference between the rigorous and the classical solution in the range of E_1/E_2 from 2 to 40 is 6.5% (rigorous below classical). For four layers, the rigorous solution is 3% below the classical solution at $E_1/E_2 = 20$ and 4% above the classical solution at $E_1/E_2 = 3$. Of course, both the two- and four-layer shell results approach the 15% difference for isotropic shells at $E_1/E_2 = 1$. With the exception of a peaking in P/P_{CL} at low E_1/E_2, the relative axial buckling load generally increases toward the classical solution as E_1/E_2 increases. However,

for increasing E_1/E_2, the axial buckling loads approach the classical buckling loads more rapidly for long shells in Fig. 5 than for short shells in Fig. 4. Also, as the number of layers increases, the axial buckling loads approach the classical buckling loads more rapidly for long shells than for short shells.

A distinctly different behavior is found for buckling under lateral pressure than for buckling under axial compression. Specifically, the relative lateral pressure buckling load decreases as the number of layers increases as seen for short shells in Fig. 6 (and in more results not shown). In fact, the results for an increasing number of layers approach the results for a single orthotropic layer (the limit of behavior of a cross-ply laminate as the number of layers increases). For long shells, the lateral pressure buckling loads are less than 1% below the classical buckling for two- and four-layered laminates.

Variation of G_{12}/E_2

Changing G_{12}/E_2 affects the shear stiffness A_{66} and the twisting stiffness D_{66} as is easily seen in the definitions of those stiffnesses given by Jones.[1] However, for a cross-ply laminate, the coupling stiffnesses as well as the other extensional and bending stiffnesses are unchanged. Thus, if the geometric and other mechanical properties are held constant, then the influence on the buckling load of changing the shear modulus can be evaluated. However, neither A_{66} nor D_{66} appears in the prebuckling equilibrium equations [Eq. (7) of Ref. 7]. Moreover, neither stiffness appears in a readily interpretable fashion in the equations for buckling from a rigorous prebuckling equilibrium state [Eqs. (12) and (13) of Ref. 7] or in the classical equations for buckling from a membrane prebuckling equilibrium state [Eqs. (1) and (2) of Ref. 2]. Thus, lacking both a physical explanation and a simple equation-based explanation for the dependence of the buckling load on the shear modulus, we resort to a numerical study. We use boron-epoxy with $E_1/E_2=10$ and $\nu_{12}=0.25$ as a baseline case, and we vary G_{12}/E_2 from 0.1 to 1.9 for both short and long shells under axial compression and lateral pressure.

For axial compression on a short shell, the relative buckling loads are plotted in Fig. 7. There, we see that the effect of prebuckling deformations becomes much more significant as G_{12}/E_2 increases. However, the normalization of the buckling load by the classical buckling load from a membrane prebuckling state is somewhat deceptive in this case. In fact, both the buckling load and the classical buckling load increase with increasing shear modulus (as would be imagined on the physical grounds of providing more resistance to buckling deformation). However, the buckling load increases much less rapidly than the classical buckling load, so P/P_{CL} decreases with increasing G_{12}. The same behavior occurs for long shells under axial compression. However, under lateral pressure, the influence of prebuckling effects is on the order of only 2-3% over the range of G_{12}/E_2 from 0.1 to 2. That is, prebuckling effects are essentially unchanged by changing G_{12}/E_2 when the shell is subjected to lateral pressure, but can be quite important when the shell is subjected to axial compression.

Variation of ν_{12}

Changing the major Poisson's ratio ν_{12} when all other mechanical properties are held constant affects all stiffnesses except A_{66} and D_{66}. We vary ν_{12} over the range from 0.1 to 1.9 despite the fact that we are not accustomed to seeing such high values for Poisson's ratio because of its low value for isotropic materials ($\nu<\frac{1}{2}$). However, for orthotropic materials, Lempriere[15] shows that ν can be larger than $\frac{1}{2}$ by deriving the relation

$$|\nu_{12}| < (E_1/E_2)^{1/2} \tag{1}$$

from a condition of positive stiffness and a more complicated relation from a condition of positive definiteness of the stiffness matrix. For boron-epoxy with $E_1/E_2=10$, we get $\nu_{12}<3.162$ from Eq. (1). We do not have enough mechanical property data to apply the more complicated relation, but we strongly suspect it would yield a lower bound on ν_{12} than 3.162. This claim is made because the more complicated relation leads to an upper bound of $\nu<\frac{1}{2}$ for isotropic materials, whereas Eq. (1) leads to $\nu<1$. Thus, the range of variation of ν_{12} from 0.1 to 1.9 used in this study is reasonable for determining the effect of Poisson's ratio on buckling loads when rigorous prebuckling displacements are considered.

The variation of the relative axial buckling load as a function of ν_{12} is shown in Fig. 7 for short shells ($L/r=0.7$). As ν_{12} increases, the axial buckling load increases slowly but monotonically over the range of ν_{12}. For long shells, the approach of the buckling load to the classical solution is more rapid than for short shells. Under lateral pressure, the relative buckling load also increases as ν_{12} increases, but the variation is quite small (less than 1%).

Variation of L/r

The geometric parameter L/r is varied from 0.5 to 4 for two-layer shells under axial compression and lateral pressure. Under axial compression, the relative buckling load rises from 0.90 to 0.94 as L/r goes from 0.5 to 0.7 and is approximately constant at 0.94 to 0.95 over the range $0.7<L/r<3.5$. The effects for lateral pressure are less dramatic and perhaps numerically less significant as shown in Fig. 8. This behavior is quite similar to that of isotropic shells under lateral pressure.[8]

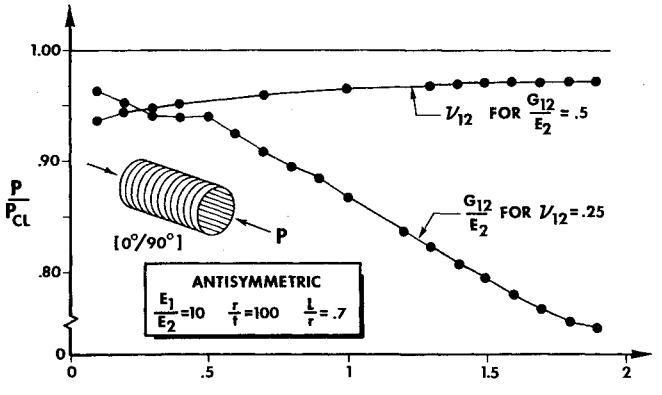

Fig. 7 Relative axial buckling loads as a function of G_{12}/E_2 and ν_{12} for two-layer antisymmetrically laminated short shells.

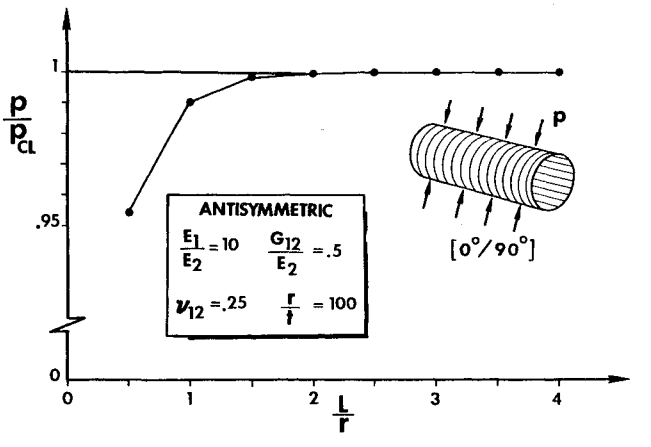

Fig. 8 Relative lateral pressure buckling loads as a function of L/r for two-layer antisymmetrically laminated shells.

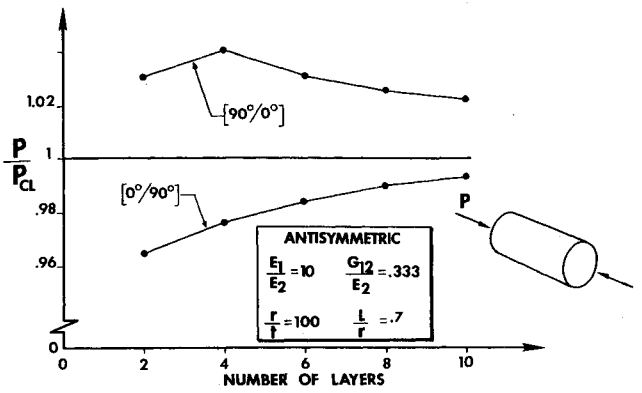

Fig. 9 Relative axial buckling loads as a function of number of layers for antisymmetrically laminated boron-epoxy short shells.

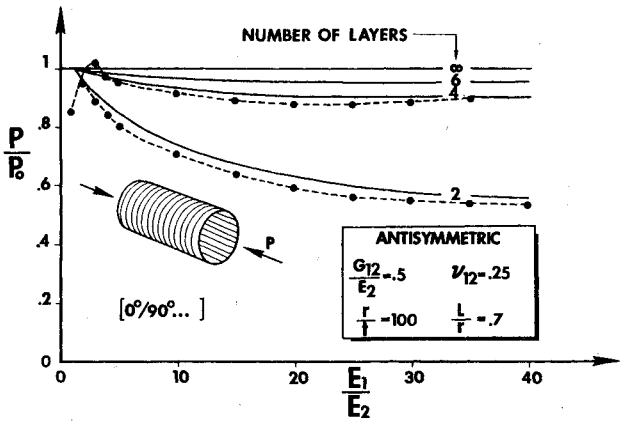

Fig. 10 Relative classical and rigorous axial buckling loads for short, antisymmetrically laminated shells.

Variation of r/t

The effect of changes in the radius-to-thickness ratio r/t on the relative axial buckling load is quite small. The biggest variation in load occurs in the range of r/t from 50 to 200 over which the relative axial buckling load increases about 1.5%. For $r/t>200$, the relative axial buckling load remains practically constant at about 0.95. No results are available for lateral pressure buckling.

Variation of Number of Layers

The variation of relative axial buckling loads for short shells made of boron-epoxy is depicted as a function of the number of layers in the laminate in Fig. 9. There, we also study the effect on the buckling load of reversing the order of lamination, i.e., having the lamination sequence [90°/0°] instead of [0°/90°] where the innermost layer is the first mentioned orientation. This switch leads to a reversal of the signs of B_{11} and B_{22}—a different kind of change than previously studied. Such a switch in lamination sequence has no effect on classical buckling loads as noted by Jones and Morgan.[2] However, when prebuckling effects are included in the analysis, the lamination sequence switch is obviously noticeable, although the ±2-4% magnitude of the differences is small from the practical standpoint. Even so, all previous results must now be regarded as having a ± nature because of the lamination switch result. In addition, the buckling loads approach the classical buckling loads from above and below as the number of layers increases. From our other results,[8] we note that this approach to the classical buckling load is more rapid for a high E_1/E_2 material like graphite-epoxy than for boron-epoxy.

Summary

We have shown the effect of considering the actual displacements in the prebuckling state on the axial or lateral pressure buckling loads of circular cylindrical shells with S2 simply supported edge boundary conditions. Normalizing the buckling loads relative to the classical buckling loads allows us to better judge the effect of the prebuckling state on the buckling loads. From these results, we can draw some general conclusions about the influence of the actual prebuckling state on the buckling loads.

Axial Buckling Load

The biggest difference between the axial buckling load and the classical axial buckling load occurs for an isotropic shell. For an orthotropic shell, i.e., with no coupling stiffnesses, the closer the elastic characteristics of the orthotropic material are to those of an isotropic material, the bigger the difference between the axial load and the classical axial buckling load. This difference decreases as the orthotropy ratio E_1/E_2 increases.

For antisymmetric cross-ply laminated shells, the buckling loads are now conveniently normalized relative to the buckling loads obtained from the classical orthotropic shell solution (P_0). In the classical orthotropic solution, only membrane prebuckling deformations are considered, and coupling stiffnesses are ignored (leaving only the extensional and bending stiffnesses of an orthotropic material). Both of these simplifications are commonly adopted in design analysis, but their effects can be separately evaluated in the present normalization approach. The solid curves in Fig. 10 are the classical laminated shell solutions for different numbers of layers with coupling accounted for only during buckling normalized by the classical orthotropic solution (P_{CL}/P_0). The dashed curves are the rigorous solutions including coupling accounted for both before and during buckling normalized by the classical orthotropic shell solution (P/P_0). The differences between the solid curves for various numbers of layers and the ordinate $P/P_{CL}=1$ are caused by coupling induced effects on the buckling loads. These differences die out as the number of layers increases, but increase as the orthotropy ratio E_1/E_2 increases. On the other hand, the differences between the solid and dashed curves are caused by prebuckling curvature induced effects on the buckling load. These latter differences die out 1) as the orthotropy ratio increases and 2) as the number of layers increases plus, from results not shown in Fig. 10, 3) as the geometric ratio L/r increases. However, if the order of lamination is reversed from [0°/90°] to [90°/0°] (i.e., the innermost layer is changed from 0 deg to 90 deg to the x axis), then the rigorous buckling load is larger than the classical load, rather than smaller as in Fig. 10, so the dashed curves in Fig. 10 would be above the solid curves. We also observed earlier that 1) as the shear modulus G_{12} increases for a short shell, the relative axial buckling load (P/P_{CL}) decreases; 2) as the Poisson's ratio ν_{12} increases, P/P_{CL} increases; 3) as L/r increases, P/P_{CL} increases; and 4) as r/t increases, P/P_{CL} increases. Obviously, from Fig. 10, the biggest effect is that of coupling between bending and extension during buckling, whereas the influence of prebuckling curvature is quite small.

Lateral Pressure Buckling Load

The difference between the lateral pressure buckling load and the classical lateral pressure buckling load for isotropic circular cylindrical shells is about 10% at $L/r=0.5$, but dies out very rapidly as the parameter L/r increases above 1.5.(Ref. 8). The effect of actual prebuckling displacements on the lateral pressure buckling load for orthotropic materials, as with axial loads, tends to decrease as the orthotropy ratio E_1/E_2 increases. This effect dies out most rapidly for a shell in which the elastic modulus in the circumferential direction is dominant (as opposed to a lower elastic modulus in the axial direction). For a short single-layer

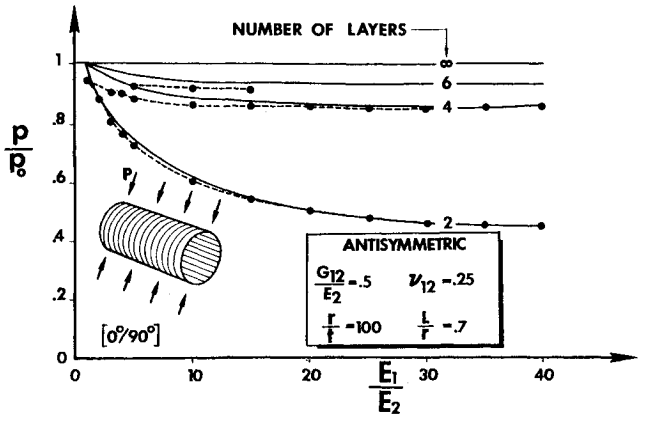

Fig. 11 Relative classical and rigorous lateral pressure buckling loads for short, antisymmetrically laminated shells

orthotropic shell, the rigorous prebuckling deformations lead to lower lateral pressure buckling loads.

For antisymmetric cross-ply laminates, the effect of prebuckling displacements increases somewhat as the number of layers increases as seen in Fig. 11, which is plotted in the same manner as Fig. 10. However, the rate of increase becomes smaller as the number of layers increases. The greatest difference is found for small values of E_1/E_2. This difference vanishes for long shells. We also observed earlier that changes in the shear modulus G_{12} and changes in the Poisson's ratio ν_{12} have little effect.

Concluding Remarks

The effect of rigorously determined prebuckling deformations on buckling loads is found for antisymmetric cross-ply laminated circular cylindrical shells with S2 simply supported edge boundary conditions. The buckling loads calculated are not numerically very different from the classical buckling loads in which prebuckling effects are ignored. This situation is quite different from isotropic shells for which prebuckling effects can lead to buckling loads up to 20% lower than classical buckling loads for S2 boundary conditions. Thus, the inclusion of prebuckling effects in design analysis of cross-ply laminated circular cylindrical shells is not warranted for S2 boundary conditions. We cannot make the same claim for other boundary conditions. In fact, Booton and Tennyson[16] obtain results for the effect of prebuckling deformations on buckling of axially compressed antisymmetrically laminated glass-epoxy circular cylindrical shells with clamped ends. For a $[\theta/0°/-\theta]$ laminated shell with $L^2/rt = 200$, the actual buckling loads (with rigorous prebuckling deformations) range from a few percent higher than the classical buckling loads at $\theta = 0$ deg and $\theta = 90$ deg to as much as 15% lower than the classical buckling loads at $\theta = 15$ deg. Thus, investigation of the full set of possible boundary conditions appears warranted.

Acknowledgment

This research was supported by the Air Force Office of Scientific Research/NA Air Force Systems Command, USAF, under AFOSR Grant 73-2532 and by the Brazilian government. We appreciate the patience and understanding of William J. Walker of AFOSR during this investigation.

References

[1] Jones, R. M., *Mechanics of Composite Materials*, McGraw-Hill, New York, 1975.

[2] Jones, R. M. and Morgan, H. S., "Buckling and Vibration of Cross-Ply Laminated Circular Cylindrical Shells," *AIAA Journal*, Vol. 13, May 1975, pp. 664-671.

[3] Whitney, J. M. and Leissa, A. W., "Analysis of Heterogeneous Anisotropic Plates," *Journal of Applied Mechanics*, Vol. 36, June 1969, pp. 261-266.

[4] Whitney, J. M. and Leissa, A. W., "Analysis of a Simply Supported Laminated Anisotropic Rectangular Plate," *AIAA Journal*, Vol. 8, Jan. 1970, pp. 28-33.

[5] Stein, M., *The Influence of Prebuckling Deformations and Stresses on the Buckling of Perfect Cylinders*, NASA TR R-190, Feb. 1964.

[6] Almroth, B. O., "Influence of Edge Conditions on the Stability of Axially Compressed Cylindrical Shells," *AIAA Journal*, Vol. 4, Jan. 1966, pp. 134-140.

[7] Jones, R. M. and Hennemann, J.C.F., "Effect of Prebuckling Deformations on Buckling of Laminated Composite Circular Cylindrical Shells," *Proceedings of the 19th AIAA/ASME Structures, Structural Dynamics, and Materials Conference*, Bethesda, Md., April 3-5, 1978, pp. 370-379.

[8] Hennemann, J.C.F., "Effect of Prebuckling Deformations on Buckling of Laminated Composite Circular Cylindrical Shells," Ph.D. Dissertation, Dept. of Civil and Mechancial Engineering, Southern Methodist University, Dallas, Texas, July 1975 (available from Xerox University Microfilms International, 100 N. Zeeb Road, Ann Arbor, Michigan 48106 as Order No. 75-29,143).

[9] Bushnell, D., Almroth, B. O., and Sobel, L. H., *Buckling of Shells of Revolution with Various Wall Constructions, Vol. 2—Basic Equations and Method of Solution*, Lockheed Missiles and Space Co., Sunnyvale, Calif., NASA CR-1050, May 1968.

[10] Cohen, G. A., "Computer Analysis of Ring-Stiffened Shells of Revolution," NASA CR-2116, 1973.

[11] Kalnis, A., "Static, Free Vibration, and Stability Analysis of Thin, Elastic Shells of Revolution," Lehigh University, Bethlehem, Pa., Air Force Flight Dynamics Laboratory, Wright-Patterson Air Force Base, Ohio, AFFDL-TR-68-144, Oct. 1968.

[12] Svalbonas, V., *Numerical Analysis of Shells, Volume I, Unsymmetric Analysis of Orthotropic Reinforced Shells of Revolution*, NASA-CR-61299, Sept. 1969.

[13] von Kármán, T. and Tsien, H.-S., "The Buckling of Thin Cylindrical Shells Under Axial Compression," *Journal of the Aeronautical Sciences*, Vol. 8, June 1941, pp. 303-312.

[14] Brush, D. O. and Almroth, B. O., *Buckling of Bars, Plates, and Shells*, McGraw-Hill, New York, 1975.

[15] Lempriere, B. M., "Poisson's Ratio in Orthotropic Materials," *AIAA Journal*, Vol. 6, Nov. 1968, pp. 2226-2227.

[16] Booton, M. and Tennyson, R. C., "Buckling of Imperfect Anisotropic Circular Cylinders Under Combined Loading," *AIAA Journal*, Vol. 17, March 1979, pp. 278-287.